ELSEVIER

Journal of Power Sources 103 (2002) 173–179

JOURNAL OF POWER SOURCES

www.elsevier.com/locate/jpowsour

The mechanisms for the growth of the anodic Pb(II) oxides films formed on Pb–Sb and Pb–Sn alloys in sulfuric acid solution

Hou-Tian Liu*, Chun-Xiao Yang, Hai-He Liang, Jiong Yang, Wei-Fang Zhou

Chemistry Department, Fudan University, Shanghai 200433, PR China

Received 18 December 2000; received in revised form 11 June 2001; accepted 18 June 2001

Abstract

The anodic Pb(II) films formed on Pb, Pb–Sb and Pb–Sn alloys at 0.9 V (versus Hg/Hg_2SO_4) in 4.5 mol/l H_2SO_4 solution for 1 h were studied using alternating current (ac) impedance, open circuit decay curve and linear sweep voltammetry methods. Our research group has obtained the thickness of the anodic PbO film on Pb from the photocurrent measurement and proved that the resistance of the anodic PbO film is close to that of the interstitial liquid among the PbO particles in the film, from which it was inferred that the anodic PbO film grows via the dissolution–precipitation mechanism. It was concluded from the experimental results that (1) the films on Pb–Sb and Pb–Sn alloys also grow via the dissolution–precipitation mechanism, and the interstitial liquid may serve as the major passage for ion transportation during the film growth, (2) Sn facilitates the mechanism of oxidation of the surface layer of PbO particles to PbO_{1+x} ($0 < x < 1$), (3) the influence of Sb to facilitate the growth of PbO_{1+x} is smaller than that of Sn, but the doping effect of Sb(III) in the PbO crystals is more remarkable, (4) Sn increases the porosity of the anodic PbO film remarkably. All of the above effects decrease the specific resistance of the films.

Keywords: Anodic PbO film; Dissolution–precipitation mechanism; The ac impedance; Lead–antimony alloy; Lead–tin alloy

1. Introduction

Antimony and tin are the important additive metals of the positive grid of the lead-acid batteries. There have been a lot of research works on the effects of antimony and tin to the electrochemical behavior of the positive grid [1–6]. However, the mechanisms of the effects have still not been fully understood for the complexity of the growth mechanism and the composition of the anodic films formed on lead and lead alloys in sulfuric acid solution. The growth of the anodic PbO film has two possible mechanisms. One is a dissolution–precipitation mechanism, another is a solid-state mechanism [7]. Most of the explanations on the effects were based on the solid-state mechanism [8,9]. However, the new results of our group show that (1) the anodic PbO film grows on Pb via a dissolution–precipitation mechanism, (2) the film is composed of PbO particles, and the interstitial liquid serves as the major passage for ion transportation during the film growth, (3) the resistance of the film is close to that of the interstitial liquid among the PbO particles in the film [10]. In the present case, the ions formed by the dissolution of PbO, Sb_2O_3 and SnO in the solution of $pH = 9$ are $PbOOH^-$, SbO_2^- and $SnOOH^-$, respectively. The saturated solubility values of SbO_2^- and $SnOOH^-$ are close to that of $PbOOH^-$ at $pH = 9$ and 25°C [11–13]. Thus, when the film grows via the dissolution–precipitation mechanism, the anodic Pb(II) film containing Sb(III) or Sn(II) may be formed through the co-precipitation of these ions [14]. Through this process both Sb and Sn affect the electrochemical behavior of the positive grid. These will be discussed in the present work.

2. Experimental

The electrolyte was 4.5 mol/l H_2SO_4 solution prepared from AR grade sulfuric acid and distilled water. Pb, Pb–1.0 at.%Sn and Pb–1.0 at.%Sb alloys were used as the working electrodes. Pb–1.0 at.%Sn and Pb–1.0 at.%Sb alloys were prepared using Pb (99.999%), Sn (99.9%) and Sb (99.9%). A Pt plate served as the counter electrode. The reference electrode was the Hg/Hg_2SO_4 electrode containing the same electrolyte as that in the test cell. All potentials reported here are referred to the Hg/Hg_2SO_4 reference electrode.

The surface of the lead electrode was mechanically polished with emery paper of successively decreasing grain

* Corresponding author. Fax: +86-21-6564-1740.
E-mail address: htliu@fudan.edu.cn (H.-T. Liu).

0378-7753/02/$ – see front matter
PII: S0378-7753(01)00839-4

size down to about 10 μm. The electrode was then rinsed with distilled water, and placed into the cell. Before anodizing, a cathodic polarization at −1.2 V for 20 min was performed to remove any oxidation products formed during the pretreatment. The anodic film studied in the present work was grown on the working electrodes for 1 h in 4.5 mol/l H_2SO_4 solution at 0.9 V, the potential near that of the positive grid of lead/acid batteries at deep-discharge.

The real part of the alternating current (ac) impedance (Z') varied with potential (E), cyclic voltammogram (CV) and open circuit decay (OCD) curve were measured by using a CHI-660 electrochemistry work station.

The linear sweep voltammetry (LSV) was carried out by using an EG&G PARC 273 potentiostat/galvanostat controlled by an EG&G PARC 270 software.

The ac impedance measurements were carried out by using a potentiostat/galvanostat (EG&G PARC 273), a two-phase lock-in analyzer (EG&G PARC 5208), and an ac impedance software (EG&G PARC 378). The amplitude of the ac signal was 5 mV. The frequency range was between 1×10^3 and 1×10^5 Hz. The electrochemical impedance spectra were analyzed using an EG&G PARC EQUIVCRT impedance modelling software.

All experiments were carried out at 25 ± 2°C.

3. Results and discussion

3.1. Z' versus E and OCD curves

Z' versus E curves for the anodic films formed on Pb, Pb–Sn and Pb–Sb electrodes at 0.9 V in 4.5 mol/l H_2SO_4 solution are shown in Fig. 1. It can be found that both Sn and Sb decrease the value of Z'. The Z' peaks, C1 (−0.58), C2 (−0.67) and C3(−0.73 V), appear in the curves for Pb–1.0 at.%Sn and Pb–1.0 at.%Sb electrodes at $E < -0.50$ V, but it does not appear in the curve for Pb electrode. Peak C1 may correspond to the reduction of Sb(III) [15], and to the cathodic peak F (−0.58 V) in the LSV curve for Pb–1.0 at.%Sb electrode in Fig. 2. Peaks C2 and C3 may correspond to the reduction of PbO_{1+x} ($0 < x < 1$) on Pb–1.0 at.%Sb and Pb–1.0 at.%Sn, respectively. The appearance of peak C1 may be due to the existence of two forms of Sb(III) in the anodic film. The anodic Pb(II) film grows via the dissolution–precipitation mechanism, so some Sb(III) may be doped into the PbO crystals and the other can form Sb_2O_3 crystals through the co-precipitation as discussed above (but if the anodic Pb(II) film grows via the solid-state mechanism, the Sb_2O_3 particles would hardly be formed, for the uniform distribution of Sb atoms in the Pb substrate and the uniform diffusion of oxygen into the film). The anodic film becomes an n-type semiconductor for the doping of Sb(III) into the PbO crystals, and as a result Sb decreases the specific resistance of the film [5]. The reduction of the doped Sb(III), earlier than that of Sb_2O_3 particles, increases the specific resistance of the film, so does the value of Z'. The reduction of the Sb_2O_3 particles to Sb decreases the specific resistance of the film and so does the value of Z'. This leads to the appearance of peak C1. For peaks C2 and C3, they may be due to the increase in the specific resistance of the PbO_{1+x} with decreasing of the x value [16]. The reduction of PbO_{1+x} to PbO will increase the resistance of the film, but the following reduction of PbO to Pb will decrease the resistance of the film. This makes the formation of peaks C2 and C3.

The existence of the PbO_{1+x} in the anodic film can be demonstrated through the OCD curves in Fig. 3 and Fig. 4. Two Pb–1.0 at.%Sn electrodes were anodized at 0.9 V for 1 h, then followed by cathodic reduction using LSV ($v = 1$ mV/s) to −0.50 V (the start potential of the Z' peak, the potential of A as shown in the curve b of Fig. 1) and −0.73 V (the peak potential of the Z' peak, the potential of B

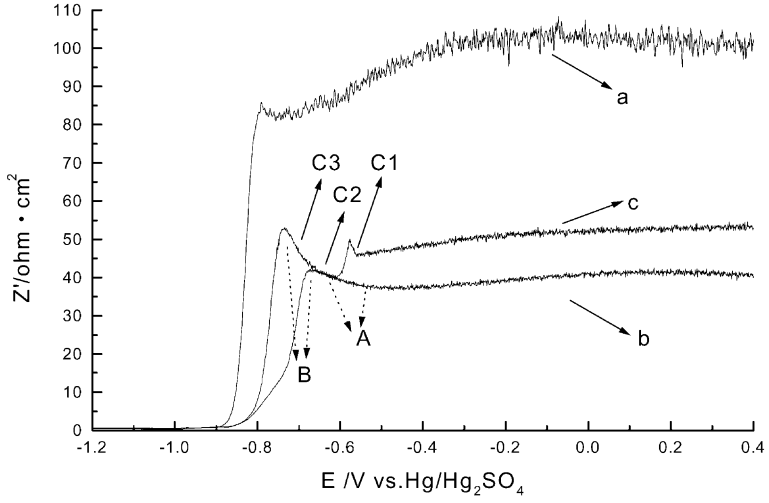

Fig. 1. The real part of the impedance (Z') vs. E plots for the anodic films formed on Pb, Pb–1.0 at.%Sn and Pb–1.0 at.%Sb at 0.9 V for 1 h, $f = 1000$ Hz, scan rate $v = 1$ mV/s, scan range 0.9 to −1.2 V (0.9–0.4 V is not shown in the figure): (a) Pb; (b) Pb–1.0 at.%Sn; (c) Pb–1.0 at.%Sb.

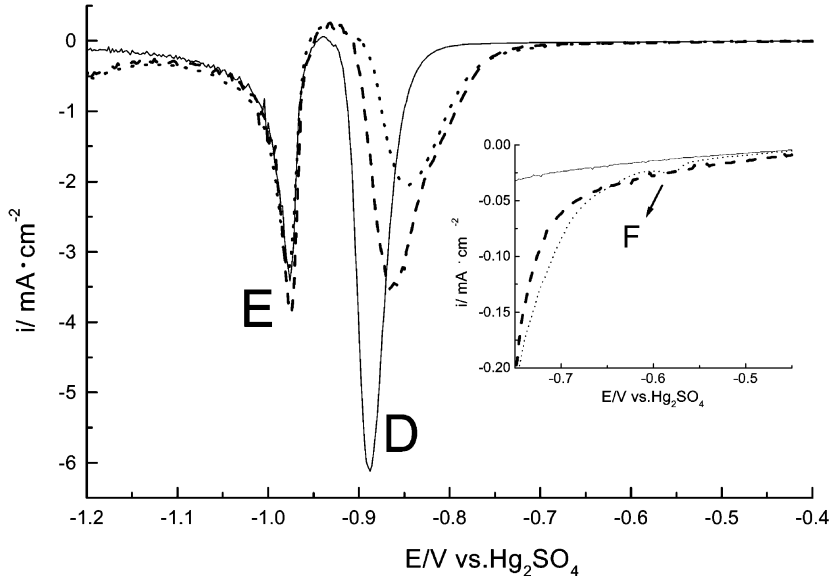

Fig. 2. LSV plots for the anodic films formed on Pb, Pb–1.0 at.%Sn and Pb–1.0 at.%Sb at 0.9 V for 1 h, scan rate $v = 1$ mV/s, scan range 0.9 to −1.2 V (0.9 to −0.4 V is not shown in the figure): (—) Pb; (- - -) Pb–1.0 at.%Sn; (···) Pb–1.0 at.%Sb.

as shown in the curve b of Fig. 1), respectively, and finally the OCD curves were measured, as shown in Fig. 3. Similarly, two Pb–1.0 at.%Sb electrodes were anodized at 0.9 V for 1 h, then followed by cathodic reduction using LSV ($v = 1$ mV/s) to −0.61 V (the start potential of the Z' peak, the potential of A as shown in the curve c of Fig. 1) and −0.67 V (the peak potential of the Z' peak, the potential of B as shown in the curve c of Fig. 1), respectively, and finally the OCD curves were measured, as shown in Fig. 4.

For the Pb–1.0 at.%Sn electrode, the PbO_{1+x} in the film is still not reduced at the start potential of the Z' peak C3 (A as shown in the curve b of Fig. 1, −0.50 V), so the steady potential should be higher than that of the equilibrium potential of Pb|PbO|$PbSO_4$. However, it should be close to the equilibrium potential of Pb|PbO|$PbSO_4$ when the circuit is opened at the peak potential of the Z' peak C3 (B as shown in the curve b of Fig. 1, −0.73 V), where the PbO_{1+x} in the film has been reduced to PbO. Fig. 3 shows that the steady potential is −0.36 V for the circuit opening at B. This potential can be thought as the steady potential of the anodic PbO film (containing Sn) formed on the Pb–1.0 at.%Sn electrode (the equilibrium potential of the anodic PbO film formed on pure lead electrode has been estimated to be −0.32 V [9], which is close to this steady potential). If the circuit is opened at A, the open circuit potential will reach the climax, −0.344 V, then slowly decay until the

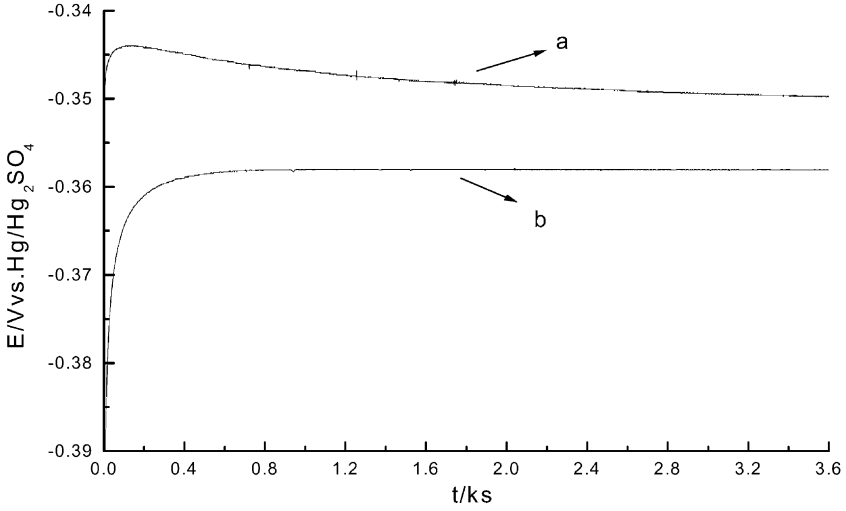

Fig. 3. Open circuit decay curves for Pb–1.0 at.%Sn anodized at 0.9 V for 1 h, followed by cathodic reduction using LSV ($v = 1$ mV/s) to −0.50 and −0.73 V, respectively, then in open circuit: (a) −0.50; (b) −0.73 V.

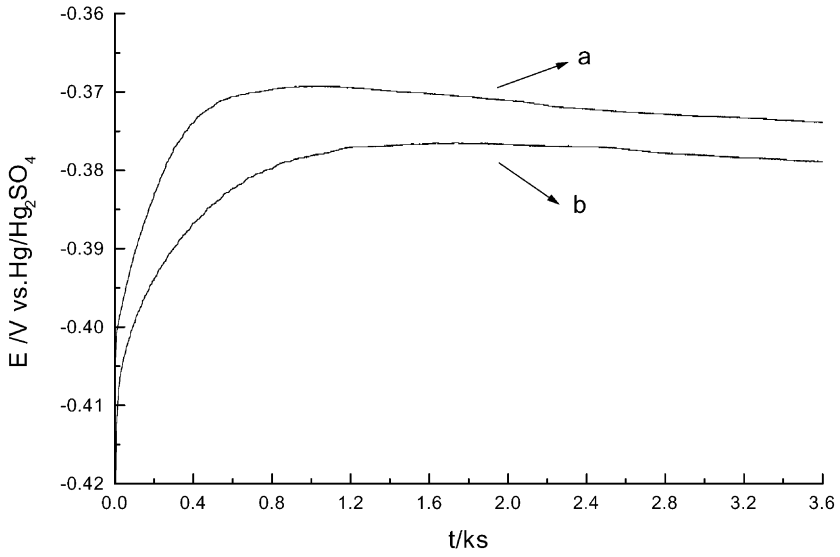

Fig. 4. Open circuit decay curves for Pb–1.0 at.%Sb anodized at 0.9 V for 1 h, followed by cathodic reduction using LSV ($v = 1$ mV/s) to −0.61 and −0.67 V, respectively, then in open circuit: (a) −0.61; (b) −0.67 V.

steady potential, −0.35 V, which is 10 mV higher than the above steady potential, −0.36 V. This shows that the potential of PbO_{1+x} is higher than that of PbO, because its chemical potential is higher than that of PbO for its more oxygen content. Therefore, the Z' peak C3 in Fig. 1 corresponds to the reduction of the PbO_{1+x}.

For the Pb–1.0 at.%Sb electrode, the PbO_{1+x} in the film is still not reduced at the start potential of the Z' peak C2 (A in the curve c of Fig. 1, −0.61 V), and so the steady potential should be higher than the equilibrium potential of Pb|PbO|$PbSO_4$. However, it should be close to the equilibrium potential of Pb|PbO|$PbSO_4$ when the circuit is opened at the peak potential of the Z' peak C2 (B in the curve c of Fig. 1, −0.67 V), where the PbO_{1+x} in the film has been reduced to the PbO. Fig. 4 shows that the steady potential is −0.38 V for the circuit opening at B. The potential can be thought as the steady potential of the anodic PbO film (containing Sb) formed on the Pb–1.0 at.%Sb electrode (which is lower than the above steady potential of Pb–Sn electrode. This may be due to the film containing Sb_2O_3. For the equilibrium potential of Sb/Sb_2O_3 is −0.42 V [11], lower than that of Pb/PbO). If the circuit is opened at point A, the open circuit potential will reach the climax, −0.369 V, then slowly decay, which is 10 mV higher than the above steady potential, −0.38 V. This shows that the potential of PbO_{1+x} is higher than that of PbO, because its chemical potential is higher than that of PbO for its more oxygen content. Therefore, the Z' peak C2 in Fig. 1 also corresponds to the reduction of the PbO_{1+x}.

Fig. 1 shows that the Z' peak corresponding to the reduction of PbO_{1+x}, does not appear in the curve of Pb electrode.

All of the above results show that Sn and Sb facilitate the process of oxidation of the surface layer of the PbO particles to PbO_{1+x}.

3.2. LSV

Fig. 2 shows the LSV curves for Pb, Pb–1.0 at.%Sn and Pb–1.0 at.%Sb electrodes. Peaks D (−0.89, −0.87 and −0.85 V) corresponds to the reduction of the Pb(II) oxides in the anodic films, and peaks E (−0.98, −0.97 and −0.98 V) to the reduction of $PbSO_4$. Peak F (−0.58 V) corresponds to the reduction of Sb_2O_3 [15]. The reduction potential of the PbO_{1+x} decreases with the x values during the reduction of the PbO_{1+x}. So no sharp reduction peaks appear in the LSV curves. According to the range of the reduction potential of PbO_{1+x} in Fig. 1, the reduction charge (Q_{AB}) of PbO_{1+x} can be calculated, as shown in Table 1.

According to the reduction charges Q_D of the peak D of the LSV curves in Fig. 2 and the reduction charges Q_{AB} (Table 1), it can be found that the quantity of the PbO_{1+x} in the anodic film is small (the Q_{AB}/Q_D values are <4%) (Table 2). Table 2 shows that the Q_{AB}/Q_D value of Pb–Sn

Table 1
Reduction charges Q_{AB} for PbO_{1+x} in the anodic films formed on Pb–1.0 at.%Sn and Pb–1.0 at.%Sb at 0.9 V for 1 h

Electrode	Reduction potential range of PbO_{1+x} (V)	Reduction charges Q_{AB} (mC/cm^2)
Pb–1.0 at.%Sn	−0.50 to −0.73	8.4
Pb–1.0 at.%Sb	−0.61 to −0.67	2.1

Table 2
Q_{AB} and Q_D

	Pb	Pb–1.0 at.%Sn	Pb–1.0 at.%Sb
Q_{AB} (mC/cm^2)	0	8.4	2.1
Q_D (mC/cm^2)	253	270	170
Q_{AB}/Q_D	0	0.031	0.012

Table 3
Reduction charges Q_L, and Q_D

	Pb (−0.86 V)[a]	Pb–1.0 at.%Sn (−0.81 V)[a]	Pb–1.0 at.%Sb (−0.80 V)[a]
Q_L (mC/cm^2)	37.0	55.5	38.3
Q_D (mC/cm^2)	253	270	170
Q_L/Q_D	0.146	0.206	0.225

[a] At this potential Z' reaches 5 Ω cm^2.

alloy is more than that of Pb–Sb alloy. Thus, Pb–Sn shows more favor to the formation of PbO_{1+x}. If the anodic film grows via a solid-state mechanism, the reduction of so small quantity of PbO_{1+x}, as discussed above, could not remarkably affect the Z' value of the anodic film, for the resistance of the oxides in the film are in series. However, if the anodic film grows via a dissolution–precipitation mechanism, the surface layer of the PbO particle may be oxidized to PbO_{1+x}. The resistance of the PbO particles covered with PbO_{1+x} may be much lower than that of the original PbO particles, even close to that of the interstitial liquid. Therefore, the reduction of PbO_{1+x} to PbO can remarkably affect the resistance of the film.

Figs. 1 and 2 show that the Z' values decreases greatly for reducing only a small quantity of the anodic films. For example, when the potential of the LSV is swept to the potential at which Z' is only 5 Ω cm^2 (lowering of ca. 87% of the Z' value at B in Fig. 1), but the quantity of the charges for the reduction (Q_L) is <23% of that of peak D in Fig. 2, as shown in Table 3. This obviously does not conform with the solid-state mechanism, because according to the solid-state mechanism the decreasing value of Z' should nearly be in direct proportion to the reduction charges for the anodic film. In fact, this is not true in the present work. If the films grow via the dissolution–precipitation mechanism, the surface layer of the oxide particles would be first reduced, then the oxide particles would be covered with a layer of good conductor Pb. Apparently, it can cause the resistance of the anodic film greatly decreased and the required reduction charges can be only a small portion of Q_D.

3.3. EIS

When the potential of the anodic oxidation for lead in sulfuric acid solution is in the PbO potential region (−0.40 to 0.95 V) [17], a complex composition of the anodic film on the lead electrode will be obtained, i.e. Pb/PbO/3PbO·PbSO$_4$·H$_2$O/PbO·PbSO$_4$/PbSO$_4$, with PbO, PbO·PbSO$_4$, and PbSO$_4$ as the major components [10,18].

Our research group [10] has obtained the thickness of the anodic PbO film from the photocurrent measurement and proved that the resistance of the anodic PbO film is close to that of the interstitial liquid among the PbO particles in the film, from which it was inferred that the anodic PbO film grows via the dissolution–precipitation mechanism.

The equivalent circuit for analysis of the impedance data is shown in Fig. 5 [10], where R1 stands for the resistance of the electrolyte, R2 and C3 are the resistance and capacitance of the anodic film containing PbSO$_4$ and PbO·PbSO$_4$, respectively, R5 and C4 are the resistance and capacitance of the anodic PbO film, respectively, R6 stands for the polarization resistance, and C7 is the capacitance of the double layer. In this equivalent circuit the resistance and capacitance of the anodic PbO film are separated from those of the other components of the anodic film.

The major components of the anodic films formed on the Pb–Sn and Pb–Sb alloys are the same as that formed on Pb. Therefore, the equivalent circuit as shown in Fig. 5 is also used for the analysis of the impedance data of the films formed on Pb–1.0 at.%Sn and Pb–1.0 at.%Sb alloys.

The Nyquist plots for the anodic films are depicted in Fig. 6. It can be found that the simulated plots fit the experimental plots well.

Table 4 lists the parameters in the equivalent circuit.

The values of the parameters of Pb–1.0 at.%Sn and Pb–1.0 at.%Sb shown in Table 4 are close to those of Pb, so the anodic films formed on Pb–1.0 at.%Sn and Pb–1.0 at.%Sb also grow via the same mechanism for that on Pb, i.e. the dissolution–precipitation mechanism.

According to the dissolution–precipitation mechanism, the decrease of the resistance of the PbO film formed on Pb–Sn alloy (R5) may be due to two reasons (1) the resistance of the solid phase (PbO particles) decreases for the oxidation of the surface layer of the PbO particles to PbO_{1+x}, whose specific resistance is smaller than that of PbO, (2) the additive Sn increases the porosity of the film (as inferred from the increase of double layer capacitance (C7) and so decreases the resistance of the liquid phase (interstitial solution among the PbO particles).

According to the dissolution–precipitation mechanism, the decrease of the resistance of the PbO film formed on Pb–Sb alloy (R5) may be due to two reasons (1) the doping of

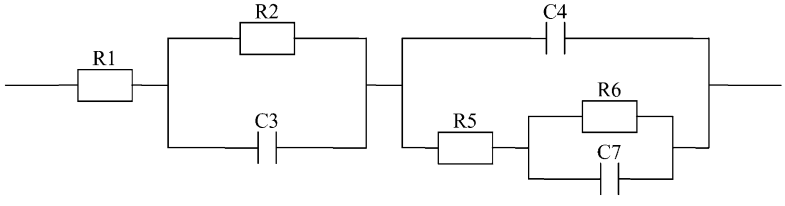

Fig. 5. The equivalent circuit of the anodic film [10].

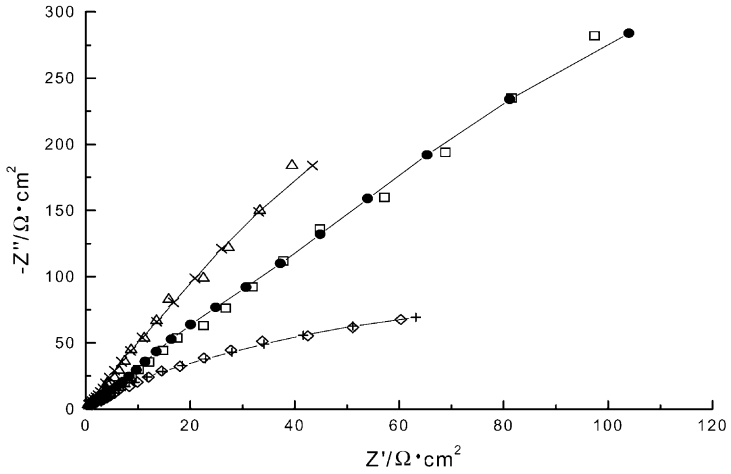

Fig. 6. The Nyquist plots for the anodic films formed on Pb, Pb–1.0 at.%Sn and Pb–1.0 at.%Sb at 0.9 V for 1 h: (□) experimental for Pb; (●) simulated for Pb; (△) experimental for Pb–1.0 at.%Sb; (— × —) simulated for Pb–1.0 at.%Sb; (◇) experimental for Pb–1.0 at.%Sn; (— + —) simulated for Pb–1.0 at.%Sn.

Sb(III) decreases the resistance of the solid phase (PbO particles), (2) the oxidation of the surface layer of the PbO particles to PbO_{1+x}, whose specific resistance is smaller than that of PbO, also decreases the resistance of the solid phase.

The induction period of the growth of *o*-PbO is shorter than that of *t*-PbO and the additive Sb can decrease the induction period of *o*-PbO [14]. This may be due to the *o*-PbO and *o*-Sb_2O_3 crystals formed through co-precipitation both belonging to the orthorhombic system. And their belonging to the same system leads to the porosity of the anodic film formed on Pb–1.0 at.%Sb electrode close to that of Pb. However, SnO crystals belong to the tetragonal system, not isomorphic with *o*-PbO crystals, so the porosity of the anodic film formed on Pb–1.0 at.%Sn electrode is larger than that on Pb (Table 4).

As shown above, the anodic films formed on Pb–Sn and Pb–Sb alloys at 0.9 V grow via the dissolution–precipitation mechanism, the interstitial liquid among the PbO particles may serve as the major passage for ion transportation during the film growth, and the surface layer of the PbO particles can be oxidized to PbO_{1+x}. The formation of PbO_{1+x} may be due to the larger bond energy of SnO and Sb_2O_3 (the values of the dissociation heat of SnO (g) = Sn (g)+O (g), SbO (g)=Sb(g) + O (g) and PbO(g) = Pb (g) + O (g) are 527, 410 and 372 kJ/mol, respectively) [19]. This makes the following reaction easier to happen on the surface of the SnO and Sb_2O_3 crystals [20].

$$H_2O \rightarrow O_{ad} + 2H^+ + 2e^-$$

This causes the concentration of O_{ad} higher on the surfaces of SbO and Sb_2O_3 crystals, which favors the diffusion of O_{ad} to the surface of the PbO particles and growth of PbO_{1+x}.

The CV curves of the anodic films formed on Pb, Pb–1.0 at.%Sn and Pb–1.0 at.%Sb are compared as shown in Fig. 7. Fig. 7 shows that the amount of the evolved oxygen and the current density for the growth of PbO_2 on the anodic films formed on Pb–1.0 at.%Sn and Pb–1.0 at.%Sb are much higher than those on Pb. Moreover, the differences between the charges for the anodic oxidation and those for the cathodic reduction, of Pb, Pb–1.0 at.%Sn and Pb–1.0 at.%Sb electrodes in Fig. 7 are 0.248, 0.328 and 0.386 C/cm^2, respectively. The differences are correlated mainly with the oxygen evolution. Hence, the oxygen evolution overpotentials of the anodic films formed on Pb–1.0 at.%Sn and Pb–1.0 at.%Sb are lower than that on Pb. Then the amounts of O_{ad} produced on the anodic film formed on Pb–1.0 at.%Sn and Pb–1.0 at.%Sb are both larger than that on Pb. This favors the combination of O_{ad}, evolution of O_2, growth of PbO_2 and oxidization of PbO to PbO_{1+x}. This difference for the Pb–Sn alloy is less than that for the Pb–Sb alloy, because the adsorption strength of O_{ad} on the anodic film formed on Pb–1.0 at.%Sn is stronger than that of Pb–1.0 at.%Sb (for the bond energy of SnO is much higher than that of Sb_2O_3). It favors the diffusion of O_{ad} to PbO, and so does the growth of PbO_{1+x} for the film on Pb–Sn than that on Pb–Sb, but makes less evolution of oxygen for the film on Pb–Sn than that on Pb–Sb.

Table 4
R2, C3, C4, R5, R6, and C7 for Pb, Pb–0.3 at.%Sn, Pb–1.0 at.%Sn

Electrode	R2 (Ω cm^2)	C3 (μF/cm^2)	C4 (μF/cm^2)	R5 (Ω cm^2)	R6 (kΩ cm^2)	C7 (μF/cm^2)
Pb	38	1.1	0.30	34	1.3	0.26
Pb–1.0 at.%Sb,	15.2	3.18	0.556	21.4	1.23	0.32
Pb–1.0 at.%Sn	23.4	1.80	0.635	8.71	0.14	1.29

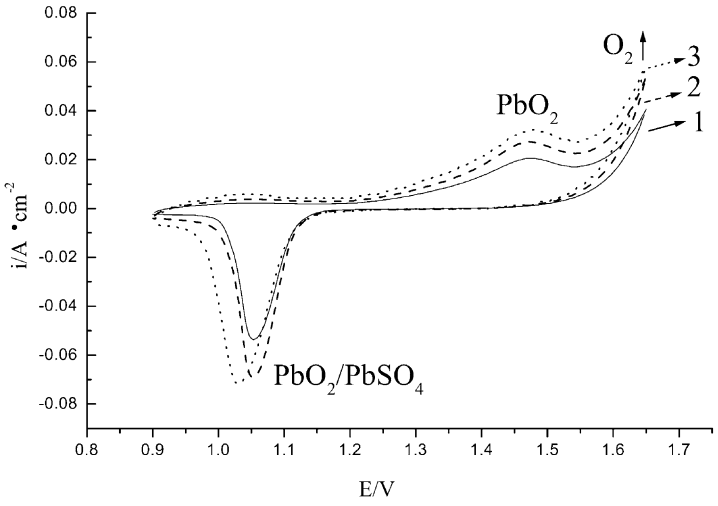

Fig. 7. Cyclic voltammograms at 30th cycle for Pb, Pb–1.0 at.%Sn and Pb–1.0 at.%Sb in 4.5 mol/l H_2SO_4, scan rate 20 mV/s, scan range 0.9–1.65 V. (1) Pb; (2) Pb–1.0 at.%Sn; (3) Pb–1.0 at.%Sb.

4. Conclusions

1. The films on Pb–Sb and Pb–Sn alloys also grow via the dissolution–precipitation mechanism, and the interstitial liquid may serve as the major passage for ion transportation during the film growth.
2. Sn facilitates the mechanism of oxidation of the surface layer of PbO particles to PbO_{1+x} ($0 < x < 1$).
3. The influence of Sb to facilitate the growth of PbO_{1+x} is smaller than that of Sn, but the doping effect of Sb(III) in the PbO crystals is more remarkable.
4. Sn increases the porosity of the anodic PbO film remarkably.

All of the above effects decrease the specific resistance of the films.

Acknowledgements

This work was supported by the National Natural Science Foundation of China, Project no. 29873013.

References

[1] D. Pavlov, in: B.D. McNicol, D.A.J. Rand (Eds.), Power Sources for Electric Vehicles, Elsevier, Amsterdam, 1984, p. 111.
[2] H.K. Giess, The effect of tin on the charge acceptance of the positive (PbO_2) lead acid battery electrode, in: K.R. Bullock and, D. Pavlov (Eds.), Proceedings of the Electrochemical Society on Advances in Lead-Acid Batteries, Vol. 84–14, Pennington, NJ, 1984, p. 241.
[3] M. Bojinov, B. Monahov, J. Power Sources 30 (1990) 287.
[4] Z.-L. He, C. Pu, W.-F. Zhou, J. Power Sources 39 (1992) 225.
[5] C. Pu, Z.-L. He, W.-F. Zhou, J. Power Sources 39 (1992) 233.
[6] M. Bojinov, K. Solmi, G. Sundholm, Electrochim. Acta 39 (1994) 719.
[7] E. Rocca, J. Steinmetz, S. Weber, J. Electrochem. Soc. 146 (1999) 54.
[8] D. Pavlov, Electrochim. Acta 23 (1978) 845.
[9] E. Rocca, J. Steinmetz, Electrochim. Acta 44 (1999) 4611.
[10] H.-T. Liu, H.-H. Liang, J. Yang, W.-F. Zhou, Chin. J. Chem. 18 (2000) 489.
[11] A.L. Pitman, M. Pourbaix, N. de Zoubov, in: Proceedings of the Ninth Meeting of the International Committe of Electrochemical Thermodynamics and Kinetics (CITCE), Butterworths, London, 1959, p. 32.
[12] H.-T. Liu, Q.-Z. Wang, Y.-Q. Wan, W.-F. Zhou, W.-B. Cai, Electrochemistry 2 (2) (1996) 123 (in Chinese).
[13] E. Deltombe, N. de Zoubov, M. Pourbaix, in: Proceedings of the Ninth Meeting of the International Committe of Electrochemical Thermodynamics and Kinetics (CITCE), Butterworths, London, 1957, p. 217.
[14] H.-T. Liu, Q.-Z. Wang, W.-F. Zhou, W.-B. Cai, Electrochemistry 3 (1997) 2 (in Chinese).
[15] W.-F. Zhou, X.-L. Chen, Acta Chim. Sinica 43 (1985) 333 (in Chinese).
[16] M. Bojinov, K. Solmi, G. Sundholm, Electrochim. Acta 39 (5) (1994) 719.
[17] D. Pavlov, C.N. Poulieff, E. Klaja, N. Iordanov, J. Electrochem. Soc. 116 (1969) 316.
[18] J. Han, C. Pu, W.-F. Zhou, J. Electroanal. Chem. 368 (1994) 43.
[19] G.V. Samsonov (Ed.), The Oxide Handbook, 2nd Edition, Plenum Press, New York, 1982, p. 86.
[20] J. O'M. Bockris, S. Srinivasan, Fuel Cells: Their Electrochemistry, McGraw-Hill, New York, 1969, p. 331.